Polarization Effect Assessment of Sub-6 GHz Frequencies on Adult and Child Four-Layered Head Models

Sai Spandana Pudipeddi
Department of EECE
School of Technology
Gandhi Institute of Technology and Management
Deemed to be University
Visakhapatnam, India
psspandana26@gmail.com

Pappu V. Y. Jayasree
Department of EECE
School of Technology
Gandhi Institute of Technology and Management
Deemed to be University
Visakhapatnam, India
jpappu@gitam.edu

Sai Gowtham Chintala
Department of EECE
School of Technology
Gandhi Institute of Technology and Management
Deemed to be University
Visakhapatnam, India
saigowthamchintala@gmail.com

Abstract-Nowadays, with the extensive use of mobile phones, the Electromagnetic (EM) radiation penetration from Radio Frequencies (RFs), particularly into the human head, is an issue that needs resolving. Some serious biological hazards occur inside the human body due to RF radiation accumulation. The RF radiation can be minimized by embodying shielding and coating materials on the front side of the mobile handset. The novelty of the proposed work is the use of mathematical analysis in calculating the Specific Absorption Rate (SAR) absorbed by planar four-layer adult and child head models when exposed to mobile smartphone RF radiation. The variation of SAR with the Angle of Incident (AoI) of the EM wave considers Transverse Electric (TE) and Transverse Magnetic (TM) Polarization. The SAR absorption alteration with the AoI of the EM wave is calculated with the help of the shielding effectiveness parameter of the external Polyethylene Terephthalate (PET) shield coated with conductive copper (Cu) mesh, forming a laminated shield using the methodology of the transmission line method. Furthermore, the SAR variation with AoI for both human head models is calculated theoretically at Sub-6 GHz mobile frequencies of 4.5GHz and 3.6GHz. SAR of 7.41e-12 W/kg and 4.41e-11 W/kg is achieved theoretically for adult and child head models respectively, at 89° TE polarization at 4.5GHz.

Keywords- specific absorption rate; shielding effectiveness; transverse electric polarization; transverse magnetic polarization; four-layered head model

I. INTRODUCTION

Mobile handsets [1-3] are used worldwide, but their introduction brought unforeseen adverse effects. These mobile handsets emit RF energy, a kind of non-ionizing electromagnetic radiation that severely affects human head tissues during their usage. More power in the form of biogenic magnetite crystals gets deposited in the human brain at higher frequencies. The brain is a target organ for EM radiation, and the different received dosage is categorized into ionizing and non-ionizing radiation [4]. The Fifth Generation (5G) technology features high cell density and higher data transmission rates. The frequency bands 5G mobile communication uses are below 6GHz, and known as the Sub-6 GHz band and FR-2 [5]. The amount of radiation emerging from a handset and entering the brain layer is estimated using the Specific Absorption Rate (SAR) parameter [6-7]. The dependent parameters of SAR are the conductivity (σ), the mass density of human head tissues (ρ), and the tissue incident electric field (E). From the ICNIRP guidelines [8], the permissible SAR is around 2W/kg. Hence, any mobile handset causing SAR more than the allowable is unauthorized for usage.

Embodying a transparent shield material [9] with conductive coating helps reducing SAR. After incorporating a shield, the shield performance is estimated using a parameter called Shielding Effectiveness (SE). This parameter depends on the calculated Total Transmission Coefficient (TTC) using the

Transmission Line Method (TLM) for two planar four-layered head models representing humans of different age. The incoming EM radiation can be incident at any arbitrary angle. The calculation of SAR for the head models includes both TE and TM polarization of the incident EM wave. Mobile phone antenna performance and design are not examined in the current work. All SAR calculations are evaluated considering a planar four-layered head model. The planar head model in Figure 1 has four layers, namely skin, fat, bone, and brain. The considered parameters are electrical conductivity (σ), relative permittivity (ε_r) and relative permeability (μ_r).
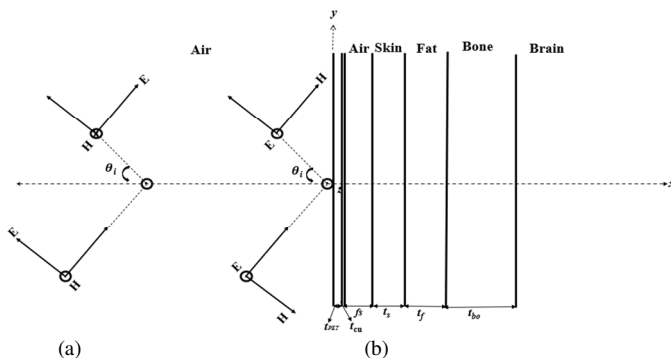
Fig. 1.   A 4-layered planar human (adult/child) head model with PET shield and Cu coating. (a) Parallel polarization, (b) perpendicular polarization of the EM wave incident on the shield surface transmitted through the head tissues.

Many researchers have worked on estimating and reducing the SAR absorbed by human adult and child head models at various mobile frequencies. Authors in [10] studied the mutual effect of interaction between mobile phones and the human head with the FDTD method to find the SAR distribution in the head near the hand-held receiver. The mobile frequencies used are 900MHz and 1800MHz. Maximum 1g and 10g averaged SAR using the FDTD method were calculated in adult and child scaled head models in [11] at GSM 900MHz and 1800MHz. The effect of a plane wave that is obliquely incident on a six-layered head structure at 900MHz and 1800MHz was analyzed mathematically by deriving the exact formula for the electric field. The SAR distribution concerning various distances between the source and head model is plotted and compared in [12]. Authors in [13] studied the SAR distributions and temperature elevation with FDTD modeling of mobile phones and WLAN networks when a plane wave is excited with an obliquely incident wave in a head model of six layers. SAR and temperature rise are calculated and studied for each head layer at 900MHz, 1800MHz, and 2400MHz at parallel and perpendicular polarization. Authors in [14] investigated the relationship between peak SAR and temperature elevation averaged over 10g of human head tissues in head models in the 1 to 300GHz range.

The novelty of the proposed work is the numerical and mathematical evaluation of SAR by utilizing the TLM taking shield parameters such as SE of different planar-aged human head models with no shield condition and with the mesh coated thin film as a laminated shield. The SAR estimation and reduction using the transparent mesh coated film is not

available in literature for mobile phone applications up to 5G frequencies. The novelty of the current work is the study of the theoretical analysis of SAR with the usage of a transparent metal mesh of minimum thickness with the TLM.

II. ANALYSIS OF SHIELDING EFFECTIVENESS OF HUMAN HEAD

A. Shielding Material and Parameters of Mesh

A shield is required to control the radiation from the handset and its design should be able to control the SAR imposed on the planar four-layered human head. This can be achieved by designing a transparent laminated shield, i.e. coating a polymer film coated with a conductive film. In the current work, the considered polymer is Polyethylene Terephthalate (PET), and the conductive coating is Copper (Cu). The combination forms a laminated mesh. The material parameters of thickness, conductivity, relative permittivity, and relative permeability are included, whereas the mesh parameters, as shown in Figure 2, are mesh spacing and width [15]. The mesh spacing and the mesh width are used to find the Cu-mesh impedance [16]. The parameters involved in the impedance equation are:

$$\eta_{Mesh} = r_{Cu-Mesh} + j x_{Cu-Mesh} \quad (1)$$

$$r_{Cu-Mesh} = \frac{1}{\sigma_{Cu}\delta\left(1-e^{-t/\delta}\right)} * \frac{g}{2a} \quad (2)$$

$$x_{Cu-Mesh} = -\frac{g}{\lambda}\left[ln\left(sin\left(\frac{\pi a}{g}\right)\right)\right] * \eta_0 \quad (3)$$

Equations (1)-(3) are used in the impedance calculation of coating film used in the analysis of the TTC from which the shielding effectiveness is derived. The shield on which the coating film is embedded is the polymer PET and its properties are shown in Table I. The impedance of the PET shield can be calculated from [17]. Therefore, the impedances of the films are calculated from (1)-(3), which help in determining the TTC. It is also necessary to resolve the tissue impedance of the human models, as described.

TABLE I.   PARAMETERS OF THE SHIELDING MATERIAL

Material	PET film	Cu mesh film
Thickness	100 μm	100 nm
Conductivity (S/m)	7.80E-13	5.96E+07
Relative permittivity	3.4	1
Relative permeability	1	1
Mesh spacing	Not applicable	300 μm
Mesh width	Not applicable	15 μm

B. Human Head Models and Tissue Parameters

In the current work, a planar four-layered head model of the adult/child human head is considered. The model properties differ significantly in their water content and tissue thickness. The tissues include the skin, fat, bone, and brain. These tissues vary in thicknesses, as shown in Table II. However, their properties vary with the operating frequency of the mobile phone device (f). The electrical conductivities (σ), relative permittivities (ε_r), and also the relative permeabilities (μ_r) of the tissues change with frequency. But since all the tissues are biological, all the relative permeabilities are equal to unity.

Also, the impedances of the tissues depend on the operating frequency. The tissue impedance is generally given by $\eta_{<k>}k$ for Skin, Fat, and Bone with (4) as the corresponding equation for impedance calculation:

$$\eta_{<k>} = (1 + j)\sqrt{\frac{\pi\mu_{<k>}f}{\sigma_{<k>}}} \quad (4)$$

From (4), the corresponding tissue relative permeability and conductivity at the mobile phone operating frequency are found by substituting all tissue impedances.
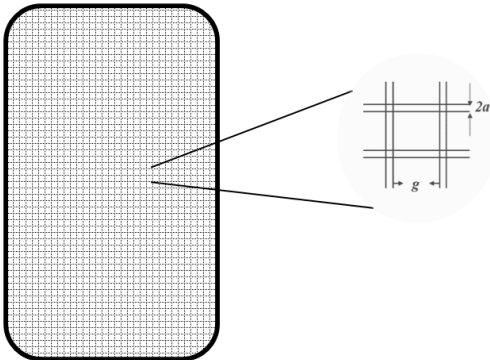
Fig. 2.   Mesh parameters of a copper coating film.

TABLE II.   TISSUE THICKNESS OF HEAD MODELS [18-19]

Tissue	Tissue thickness (mm)	
	Adult head	**Child head**
Skin	1	1
Fat	2	0.5
Bone	7	6.5
Brain	70.5	62.3

TABLE III.   ELECTRICAL CONDUCTIVITY AND PERMITTIVITY OF TISSUES WITH FREQUENCY

Frequency (GHz)	Head tissue	Electrical conductivity (S/m)	Relative permittivity
3.6	Skin	2.085	36.92
	Fat	0.161	5.1641
	Bone	0.637	10.74
	Brain	2.724	47.159
4.5	Skin	2.687	36.18
	Fat	0.212	5.0766
	Bone	0.844	10.28
	Brain	3.58	45.862

C. Effect of Polarization on the Impedance of Shield Medium and Tissues

Electromagnetic radiation can be incident over a wide range of the angle (θ). In the case of a TE/TM polarized wave, the impedances of the shield or any medium or tissue are altered by a ratio of $cos\,\theta$. The angle of incidence (θ) would range for all acute angles (0° to 90°)—the polarization effect results in different transmission coefficients than the ones considered without polarization. Therefore, a variation is introduced in the SE of the head, and the SAR is absorbed. The interpretation of SAR considering the AoI of EM wave for polarization and head models is considered. Irrespective of medium or tissues, the impedance variation with polarization is:

$$Z_{<k>} = \frac{\eta_{<k>}}{cos\,\theta}\,(for\,TE) \quad (5)$$

$$Z_{<k>} = \eta_{<k>} * cos\,\theta\,(for\,TM) \quad (6)$$

D. SE and SAR Calculations using the Transmission Line Method

During the estimation of SAR, its relatively dependent parameter SE needs to be calculated. SE can be calculated by determining the corresponding TTC (T) of the wave radiated by the TLM. The reflection coefficients at the interfaces of the tissues are calculated by taking the impedances introduced by them under TE and TM polarization. Once the total transmission coefficient is calculated through the TLM, the SE can be determined [20-21].

$$SE(dB) = -20log_{10}(T) \quad (7)$$

$$T = p\prod_{k=Skin}^{Bone}[(1 - q_{<k>}e^{-2\gamma_{<k>}l_{<k>}})]e^{-\gamma_{<k>}l_{<k>}} \quad (8)$$

$$T = p\prod_{k=PET}^{Bone}[(1 - q_{<k>}e^{-2\gamma_{<k>}l_{<k>}})]e^{-\gamma_{<k>}l_{<k>}} \quad (9)$$

The step-by-step numerical procedure to evaluate the SAR absorbed into human head is:

Step 1: The mathematical finding of the transmission coefficient T without shield and with the PET/Cu coated laminated mesh as shield is obtained from (8) and (9). k ranges from PET shield and Cu mesh coat to brain layer. $q_{<k>}$ gives the reflection coefficient at the interface of the layered medium, $\gamma_{<k>}$ is the respective propagation constant of the layered medium, and $l_{<k>}$ is the thickness of each medium.

Step 2: The SE of any barrier in terms of electric field E is:

$$SE = 20\log_{10}\left(\frac{E_i}{E_t}\right) \quad (10)$$

Step 3: The incident electric field (E_i) from (10) is obtained from the power density incident on the head from the guidelines issued by ICNIRP [8] which is 40W/m^2 for frequency greater than 2GHz.

Step 4: The transmitted electric field (E_t) into the brain can be determined from the shielding effectiveness of the human head models without shield and with the PET and Cu laminated mesh.

Step 5: Equations (7) and (11) are necessary for SAR calculation, and thus, (8) and (9) give the variation of SAR with polarization for both head models.

$$SAR = \frac{\sigma E_t{}^2}{\rho} \quad (11)$$

III.   RESULTS AND DISCUSSION

From (8), the SE from the TLM varies according to the AoI range from 0° to 90° for both TE and TM polarizations. The results are obtained by simulations in Matlab. The variations with AoI are plotted and compared. The SE and SAR calculations with changing operating frequency are listed in Tables IV and VI.

TABLE IV.   SHIELDING EFFECTIVENESS OF HUMAN HEAD MODELS IN VARIATION WITH ANGLE OF INCIDENCE AT TWO SUB- 6 GHZ FREQUENCIES

Frequency (GHz)	AoI (degrees)	Shielding effectiveness (SE in dB)							
		4-layer adult head model				4-layer child head model			
		Without shield		With PET/Cu laminated shield		Without shield		With PET/Cu laminated shield	
		TE polarization	TM polarization	TE polarization	TM polarization	TE polarization	TM polarization	TE polarization	TM polarization
3.6	0	9.83	9.83	68.75	68.75	2.46	2.46	61.34	61.34
	30	9.62	10.08	70.26	67.28	2.21	2.74	62.80	59.92
	45	9.35	10.48	72.45	65.26	1.90	3.20	64.92	57.98
	60	9	11.33	76.41	61.96	1.48	4.16	68.76	54.78
	89	8.13	31.80	127.74	36.61	0.41	25.15	119.98	29.96
4.5	0	12.30	12.30	70.87	70.87	4.72	4.72	63.02	63.02
	30	12.12	12.51	72.49	69.29	4.52	4.95	64.59	61.49
	45	11.91	12.84	74.85	67.14	4.27	5.32	66.89	59.40
	60	11.61	13.56	79.14	63.63	3.93	6.12	71.08	56.00
	89	10.90	32.69	132.24	37.55	3.08	25.55	124.37	30.40

TABLE V.   RESULT COMPARISON

Frequency range (Mhz)	SAR assessment technique	Obtained SAR absorption values (W/Kg)	Head model	Reference
900, 1800	Finite-Difference Time-Domain (FDTD)	0.037	Adult	[11]
900, 1800	FDTD	0.42 at TE polarization, 0.83 at TM polarization	Adult	[12]
900, 1800, 2400	FDTD	1.8 at TE polarization, 2 at TM polarization	Adult	[13]
3600, 4500	TLM	1.51E-06 at TE and 5.38E-05 for TM polarizations for adult model with laminated shield and 9.42E-06 for TE and 3.03E-04 for TM polarizations for child model with laminated shield.	Adult and child	Current work

TABLE VI.   SAR ABSORBED BY BRAIN IN BOTH HEAD MODELS IN TE AND TM POLARIZATION AT TWO SUB-6 GHZ FREQUENCIES

Frequency (GHz)	AoI (degrees)	SAR (W/kg)							
		4-layer adult head model				4-layer child head model			
		Without shield		With PET/Cu laminated shield		Without shield		With PET/Cu laminated shield	
		TE polarization	TM polarization	TE polarization	TM polarization	TE polarization	TM polarization	TE polarization	TM polarization
3.6	0	12.71	12.71	1.63E-05	1.63E-05	66.68	66.68	8.63E-05	8.63E-05
	30	13.34	12	1.15E-05	2.29E-05	70.63	62.52	6.17E-05	1.20E-05
	45	14.2	10.95	6.95E-06	3.64E-05	75.86	56.23	3.78E-05	1.87E-04
	60	15.39	9	2.79E-06	7.79E-05	83.56	45.08	1.56E-05	3.91E-04
	89	18.81	0.08	2.06E-11	0.027	106.91	0.36	1.18E-10	0.12
4.5	0	7.3	7.3	1.02E-05	1.02E-05	40.73	40.73	6.03E-05	6.03E-05
	30	7.61	6.97	7.00E-06	1.46E-05	42.69	38.64	4.20E-05	8.57E-05
	45	8	6.45	4.06E-06	2.40E-05	45.21	35.45	2.47E-05	1.38E-04
	60	8.56	5.46	1.51E-06	5.38E-05	48.86	29.53	9.42E-06	3.03E-04
	89	10.1	0.07	7.41E-12	2.18E-02	59.38	0.34	4.41E-11	1.10E-01
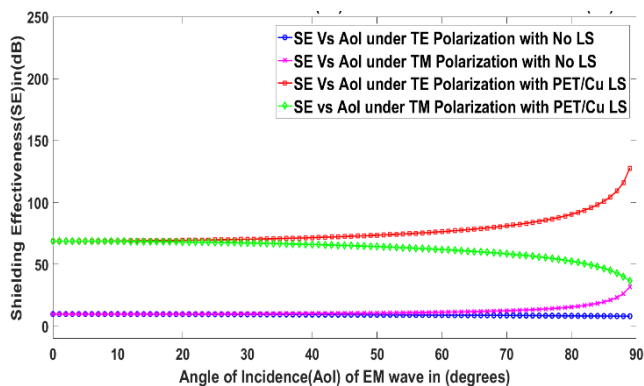
Fig. 3.   SE plot of the head without shield and PET-Cu mesh Laminated Shield (LS) for AoI in the 4-layered adult head at 3.6GHz fixed-mobile frequency for TE and TM polarization.

In Figures 3 and 4, the comparison of the SE variation with the operating frequency for a four-layered adult head is made. It is observed that at 3.6GHz, the SE values for TE polarization appear to be constant. However, they decrease drastically without the shield. With the shield, the SE values increased sharply from 30° to 89°. In the case of TM polarization without a shield, the SE values increased symmetrically about TE polarized SE values from 72° to 89°. However, it can be seen that the SE values with shield at TM polarization abruptly decrease from 30° to 89°. At 4.5GHz, the phenomenon remains the same, but the difference is that at 4.5GHz, the SE values are higher than at 3.6GHz.

Figures 5 and 6 compare the SE variation with the operating frequency of the mobile phone for the four-layered child head. At 3.6GHz, the SE values for TE polarization appear constant, but they decreased drastically without the

shield, while they increased with the shield. In the case of TM polarization and without a shield, the SE values increased symmetrically about the TE polarized SE values. We see that the SE values with the shield are more significant than those without it. Moreover, the SE values in the model of the child head are always less than in the adult head model.
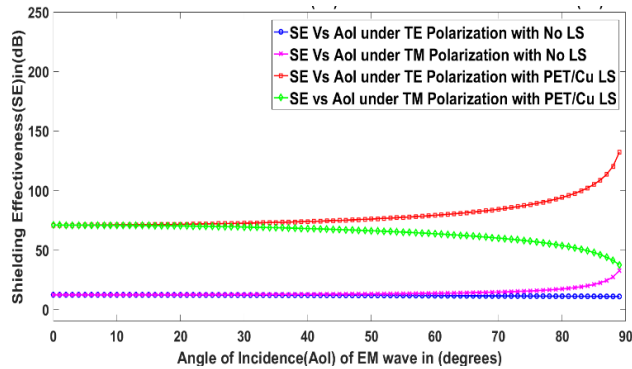
Fig. 4.   SE plot of the head without shield and PET-Cu mesh LS for AoI in the 4-layered adult head at 4.5GHz fixed-mobile frequency for TE and TM polarization.
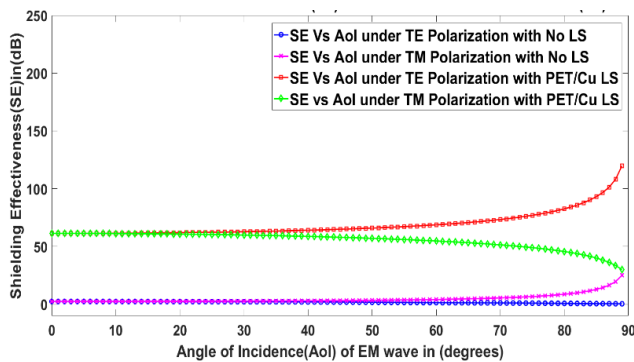
Fig. 5.   SE plot of the head without shield and PET-Cu mesh LS vs angle of incidence in the 4-layered child head model at 3.6GHz fixed-mobile frequency for TE and TM Polarization.
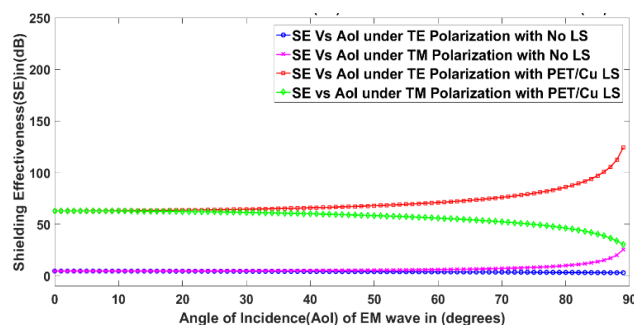
Fig. 6.   SE plot of the head without shield and with PET-Cu mesh LS vs angle of incidence in the 4-layered child head model at 4.5GHz fixed-mobile frequency for TE and TM polarization.

From Figures 3-6, for TE polarization with PET and Cu shield, the SE started to increase sharply at 35°, and for TM polarization, it abruptly decreased from 35° to 89°. The values of SE of head variation for particular angles of incidence of EM waves are listed in Table IV, and their corresponding SAR values in Table VI. It is observed from Table V that with an increase in the SE of the four-layered adult/child head with frequency, the SAR absorbed by the brain consistently decreased to a negligible level much lesser than the prescribed SAR limit. The comparison of the results of the proposed method with the existing results is exhibited in Table V.

IV.   CONCLUSION

The current paper compares the effect on human head models of the penetration of RF EM radiation for varying AoI from the sub-6 GHz operating frequency mobile phone. In TE and TM polarization, the SAR of the child model without a shield dominated over the adult model without a shield. When using a PET with a Cu laminated shield mounted on the front part of the mobile handset, the SAR is decreased in both models. Based on the operating mid-band 5G mobile smartphones and the incident angle polarization, the SAR variations are observed in both the head models without and with the laminated shield. In contrast, at the same operating frequency, for TE polarization, the SAR absorbed by the brain of the child model without a shield varied from 40.73 to 50.38W/kg for 0° to 89° angle of incidence variation. In contrast, the SAR decreased from 6E-05 to 4.41E-11W/kg with the PET and Cu lamination in TE polarization. For TM polarization and the same child head model, operating frequency, and AoI variation, the SAR decreased from 40.73 to 0.34W/kg, and with PET Cu mesh, it increased from 6.03E-05 to 0.11W/kg. Also, the minimum absorbed SAR was found at 4.5GHz for the adult head model in TE polarization at 89°, and the maximum absorbed SAR by the brain tissue was observed at 3.6GHz in the child head model in TE polarization at 89°. Therefore, the adult model absorbed more negligible radiation than the child head model with the PET/Cu mesh. However, compared to SAR without the laminated shield in a child's head, incorporating PET and Cu-based transparent film in the mobile handset has considerably decreased the SAR absorbed by the brain.

REFERENCES

[1]   D. T. T. My, H. N. B. Phuong, T. T. Huong, and B. T. M. Tu, "Design of a Four-Element Array Antenna for 5G Cellular Wireless Networks," *Engineering, Technology & Applied Science Research*, vol. 10, no. 5, pp. 6259–6263, Oct. 2020, https://doi.org/10.48084/etasr.3771.

[2]   T. Jadhav and S. Deshpande, "A Tri-band Planar Inverted-F Antenna with Complementary Split Ring Resonator and Reactive Impedance Surface for Wireless Application," *Engineering, Technology & Applied Science Research*, vol. 12, no. 1, pp. 7988–7992, Feb. 2022, https://doi.org/10.48084/etasr.4592.

[3]   S. Ghnimi, A. Nasri, and A. Gharsallah, "Study of a New Design of the Planar Inverted-F Antenna for Mobile Phone Handset Applications," *Engineering, Technology & Applied Science Research*, vol. 10, no. 1, pp. 5270–5275, Feb. 2020, https://doi.org/10.48084/etasr.3287.

[4]   D. Vatamanu and S. Miclaus, "Magnetite Particle Presence in the Human Brain: A Computational Dosimetric Study to Emphasize the Need of a Complete Assessment of the Electromagnetic Power Deposition at 3.5 GHz," *Engineering, Technology & Applied Science Research*, vol. 11, no. 5, pp. 7720–7729, Oct. 2021, https://doi.org/10.48084/etasr.4466.

[5]   D. B. Deaconescu, A. M. Buda, D. Vatamanu, and S. Miclaus, "The Dynamics of the Radiated Field Near a Mobile Phone Connected to a 4G or 5G Network," *Engineering, Technology & Applied Science Research*, vol. 12, no. 1, pp. 8101–8106, Feb. 2022, https://doi.org/10.48084/etasr.4670.

[6] H. Khan *et al.*, "Analytical Study of Specific Absorption Rate Distribution on Different Antennas Operating At 2.4 Ghz Using HFSS," *International Journal of Applied Engineering Research*, vol. 10, pp. 19855–19866, Jan. 2015.

[7] B. P. Nadh, B. T. P. Madhav, and M. S. Kumar, "Design and analysis of dual band implantable DGS antenna for medical applications," *Sadhana*, vol. 44, no. 6, May 2019, Art. no. 131, https://doi.org/10.1007/s12046-019-1099-8.

[8] International Commission on Non-Ionizing Radiation Protection, "Guidelines for Limiting Exposure to Electromagnetic Fields (100 kHz to 300 GHz)," *Health Physics*, vol. 118, no. 5, pp. 483–524, Dec. 2020, https://doi.org/10.1097/HP.0000000000001210.

[9] F. G. K. Abdulla and R. Abdulla, "A Comparative Application for Evaluating Composite Fabrics Used in Electromagnetic Shielding," *Engineering, Technology & Applied Science Research*, vol. 7, no. 6, pp. 2156–2159, Dec. 2017, https://doi.org/10.48084/etasr.1480.

[10] F. Akleman and L. Sevgi, "FDTD analysis of human head-mobile phone interaction in terms of specific absorption rate calculations and antenna design," in *IEEE-APS Conference on Antennas and Propagation for Wireless Communications (Cat. No.98EX184)*, Waltham, MA, USA, Nov. 1998, pp. 85–88, https://doi.org/10.1109/APWC.1998.730661.

[11] M. Martinez-Burdalo, A. Martin, M. Anguiano, and R. Villar, "Comparison of FDTD-calculated specific absorption rate in adults and children when using a mobile phone at 900 and 1800 MHz," *Physics in Medicine and Biology*, vol. 49, no. 2, pp. 345–354, Jan. 2004, https://doi.org/10.1088/0031-9155/49/2/011.

[12] A. A. Omar, Q. M. Bashayreh, and A. M. Al-Shamali, "Investigation of the effect of obliquely incident plane wave on a human head at 900 and 1800 MHz," *International Journal of RF and Microwave Computer-Aided Engineering*, vol. 20, no. 2, pp. 133–140, 2010, https://doi.org/10.1002/mmce.20402.

[13] A. I. Sabbah, N. I. Dib, and and M. A. Al-Nimr, "SAR and Temperature Elevation in a Multi-Layered Human Head Model Due to an Obliquely Incident Plane Wave," *Progress In Electromagnetics Research M*, vol. 13, pp. 95–108, 2010, https://doi.org/10.2528/PIERM10051502.

[14] R. Morimoto, I. Laakso, V. D. Santis, and A. Hirata, "Relationship between peak spatial-averaged specific absorption rate and peak temperature elevation in human head in frequency range of 1–30 GHz," *Physics in Medicine and Biology*, vol. 61, no. 14, pp. 5406–5425, Apr. 2016, https://doi.org/10.1088/0031-9155/61/14/5406.

[15] T. Jiubin and Y. Liu, "Frequency Dependent Model of Sheet Resistance and Effect Analysis on Shielding Effectiveness of Transparent Conductive Mesh Coatings," *Progress In Electromagnetics Research*, vol. 140, pp. 353–368, 2013, https://doi.org/10.2528/PIER13050312.

[16] S. Walia, A. K. Singh, V. S. G. Rao, S. Bose, and G. U. Kulkarni, "Metal mesh-based transparent electrodes as high-performance EMI shields," *Bulletin of Materials Science*, vol. 43, no. 1, Aug. 2020, Art. no. 187, https://doi.org/10.1007/s12034-020-02159-7.

[17] R. B. Schulz, V. C. Plantz, and D. R. Brush, "Shielding theory and practice," *IEEE Transactions on Electromagnetic Compatibility*, vol. 30, no. 3, pp. 187–201, Dec. 1988, https://doi.org/10.1109/15.3297.

[18] B. Rajagopal and L. Rajasekaran, "SAR assessment on three layered spherical human head model irradiated by mobile phone antenna," *Human-centric Computing and Information Sciences*, vol. 4, no. 1, Aug. 2014, Art. no. 10, https://doi.org/10.1186/s13673-014-0010-1.

[19] A. Drossos, V. Santomaa, and N. Kuster, "The dependence of electromagnetic energy absorption upon human head tissue composition in the frequency range of 300-3000 MHz," *IEEE Transactions on Microwave Theory and Techniques*, vol. 48, no. 11, pp. 1988–1995, Aug. 2000, https://doi.org/10.1109/22.884187.

[20] P. S. Spandana and P. V. Y. Jayasree, "Numerical Computation of SAR in Human Head with Transparent Shields Using Transmission Line Method," *Progress In Electromagnetics Research M*, vol. 105, pp. 31–45, Jul. 2021.

[21] P. K. Dutta, P. V. Y. Jayasree, and V. S. S. N. S. Baba, "SAR reduction in the modelled human head for the mobile phone using different material shields," *Human-centric Computing and Information Sciences*, vol. 6, no. 1, Apr. 2016, Art. no. 3, https://doi.org/10.1186/s13673-016-0059-0.